International Journal of Pharmaceutics 420 (2011) 180–188

Contents lists available at SciVerse ScienceDirect

International Journal of Pharmaceutics

journal homepage: www.elsevier.com/locate/ijpharm

Pharmaceutical Nanotechnology

# Enhanced bioavailability after oral and pulmonary administration of baicalein nanocrystal

Jianjun Zhang[a,1], Huixia Lv[a,1], Kun Jiang[b], Yuan Gao[b,*]

[a] Department of Pharmaceutics, China Pharmaceutical University, Nanjing 210009, PR China
[b] School of Traditional Chinese Medicine, China Pharmaceutical University, Nanjing 210009, PR China

ARTICLE INFO

*Article history:*
Received 24 May 2011
Received in revised form 4 August 2011
Accepted 16 August 2011
Available online 22 August 2011

*Keywords:*
Baicalein
Nanocrystal
Anti-solvent recrystallization
High pressure homogenization
Pulmonary administration
Bioavailability

ABSTRACT

The aim of the study was to investigate the potential of oral and pulmonary nanocrystal to enhance the bioavailability of baicalein, a bioactive flavonoid isolated from the root of *Scutellaria baicalensis* Georgi. So far, the nano-sized delivery system of baicalein and its pulmonary delivery have received no exploration. In the present investigation, the baicalein nanocrystal was prepared by anti-solvent recrystallization followed by high pressure homogenization. In vitro characterization was performed including particle size and distribution, Zeta potential, dissolution, scanning electron microscopy, differential scanning calorimetry and X-ray powder diffractometry. It was indicated that no crystalline change was observed after nanocrystal preparation. The baicalein nanocrystal containing only trace of stabilizer exhibited a significantly enhanced dissolution of baicalein. In vivo test was also carried out in rats and pharmacokinetic parameters of the baicalein crystal and the baicalein nanocrystal after gavage and pulmonary administration were compared, based on the simultaneous determination of baicalein and baicalin by high performance liquid chromatography. The mean relative bioavailability of oral baicalein nanocrystal was 1.67-fold that of oral baicalein crystal. The pulmonary baicalein nanocrystal had rapid and extensive absorption and had almost identical pharmacokinetic parameters to intravenous baicalein injection.
© 2011 Elsevier B.V. All rights reserved.

## 1. Introduction

Baicalein, the bioactive flavonoid isolated from the root of *Scutellaria baicalensis* Georgi (Yang et al., 2000) (Fig. 1), is the aglycone of baicalin and an inhibitor of CYP2C9 (Si et al., 2009), an enzyme of the cytochrome P450 system that metabolizes drugs in the body. It was reported that baicalin is poorly absorbed, but is hydrolyzed to baicalein by intestinal bacteria and then restored to its original form from the absorbed baicalein in the body (Akao et al., 2000).

In spite of the variety of pharmacological effects (Chou et al., 2003), such as anti-cancer (Li-Weber, 2009), anti-HIV (Wang et al., 2004), ant-inflammatory (Hong et al., 2002), anti-bacterial (Kubo et al., 1981) and anti-adipogenic (Lee et al., 2010) activities and relatively higher absorption than baicalin, the uses of baicalein in pharmaceutical field are still limited, due to its low water solubility (~0.1 mg/ml), extensive liver and intestinal first-pass metabolism (Zhang et al., 2005, 2007a,b) and the existence of enterohepatic circulation (Xing et al., 2005).

Baicalein is a class II (i.e., poorly water soluble and highly permeable, with $P_{app} = 1.7 \times 10^{-5}$ cm/s (Zhang et al., 2007b)) API according to the Biopharmaceutics Classification System (BCS) (Amidon et al., 1995). Few formulation approaches have been attempted to improve its oral absorption through the technique of HP-β-CD inclusion (Liu et al., 2006) or solid dispersion (Yan et al., 2008). Large amounts of cyclodextrin or polymer was used to enhance the dissolution and bioavailability through the formation of the amorphous baicalein.

Pulmonary route has gained growing attention as a potential way for delivering drugs to the systemic circulation in that the drugs would avoid the first-pass effect of the gastrointestinal tract and can be absorbed efficiently in a large lung surface area (approximately 100 $m^2$). In addition, good vascularization and the ultra-thinness of the alveolar epithelium (approximately 0.1–0.5 μm) can facilitate rapid drug absorption (Park et al., 2007).

Recently, drug nanocrystals have shown promising potential in drug delivery to offer a unique solution for the poor bioavailability of poorly water- and lipid-soluble drugs. In contrast to nanoemulsions (Collins-Gold et al., 1990) and lipid nanoparticles (Müller et al., 2011a), drug nanocrystals are particles made from almost 100% drug, stabilized by a small amount of surfactants or polymeric stabilizers (Hu et al., 2011; Mauludin et al., 2009a; Müller et al., 2011b; Shegokar and Müller, 2010; Zhang et al., 2011). Nanocrystal can be delivered via oral or pulmonary route (Kraft et al., 2004). The research on the nano-sized delivery system of baicalein is limited and pulmonary delivery received no exploration

* Corresponding author. Tel.: +86 25 83379418; fax: +86 25 83379418.
*E-mail address:* amicute@163.com (Y. Gao).
[1] These authors equally contributed to this study.

0378-5173/$ – see front matter © 2011 Elsevier B.V. All rights reserved.
doi:10.1016/j.ijpharm.2011.08.023

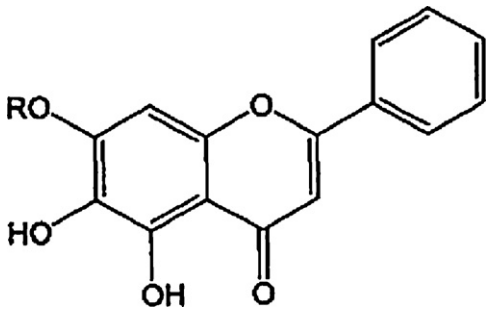


**Fig. 1.** Molecular structure of baicalin and baicalein. Baicalin: R, beta-glucopyranurosyl (molecular weight = 446.36); baicalein: R, H (molecular weight = 270.24).

so far. With the aim to increase the dissolution and bioavailability of baicalein, its nanocrystal was prepared by the anti-solvent recrystallization as a pre-treatment step followed by high pressure homogenization method. The physicochemical properties of the baicalein nanocrystal were characterized in vitro. Its relative bioavailability and absolute bioavailability after oral or pulmonary administration were evaluated in rats.

## 2. Materials and methods

### 2.1. Materials

Baicalein (purity >99.0% by HPLC) was provided by Nanjing Zelang Medical Technology Co., Ltd. (Nanjing, China). Baicalin standard was purchased from the National Institute for the Control of Pharmaceutical and Biological Products (Beijing, China). Polysorbate 80, sodium dodecyl sulphate (SLS), sodium carboxymethyl cellulose (CMC-Na) and pentobarbital sodium were purchased from Guoyao Chemical Co., Ltd. (Shanghai, China). Poloxamer188 (Lutrol®F68) and PEG400 were gifted by BASF (Ludwigshafen, Germany). Heparin sodium salt (180 IU/mg) was purchased from Sigma Chemical Co., Ltd. (St. Louis, USA). HPLC grade water was produced by a Milli-Q water purification system (Millipore Co., Ltd., Bedford, USA) and was used throughout the experiments. Other chemicals were of HPLC or analytical grade.

### 2.2. Preparation of baicalein nanocrystals

The baicalein nanocrystal was prepared by modified anti-solvent recrystallization (Zhang et al., 2009) followed by high pressure homogenization. Baicalein (800 mg), dissolved in 200 ml ethanol, was poured into 1000 ml aqueous solution containing a stabilizer (polysorbate 80 or SLS or poloxamer188, concentration at 0.1–0.5%, w/v) stirred with RW 20 digital overhead stirrer (IKA, Germany) at 1600 rpm for 5 min. The obtained suspension of microcrystalline baicalein was then homogenized by high pressure homogenization (NS 1001L, Niro Soavi S.P.A, Italy). At first, 5 cycles at 200 bar were conducted as pre-milling step, and then 10 cycles at 1000 bar were run to obtain the nanocrystal dispersion. After centrifugation using an ultracentrifuge (Hitachi himac CR 21G, Hitachi Koki Co., Ltd., Japan) at the rotate speed of 10 000 rpm for 10 min (15 °C), the upper clear liquid was removed and the remaining residue was dried in a heated vacuum desiccator at 40 °C for 24 h.

### 2.3. Particle size and zeta potential analysis

Photon correlation spectroscopy (Zetasizer 3000HSA, Malvern Instruments Ltd., Malvern, UK) was used to measure the particle size and zeta potential of the freshly precipitated microcrystals from anti-solvent recrystallization, the freshly liquid nanocrystal dispersion and the reconstituted nanocrystal upon redispersing the solid nanocrystal. To measure the particle size of reconstituted nanocrystal, ~10 mg solid nanocrystal was added into 10 ml deionized water, and then the resultant suspension was vigorously shaken by hand for 1 min. Preliminary tests showed that the PI value of particle size was $0.87 \pm 0.31$ at the solid concentration of 4 mg/ml and $0.32 \pm 0.11$ at 1 mg/ml. The decreased PI and SD suggested that the solid nanocrystal had certain particle interaction at high concentration which can result in the increase of particle size and the relatively inhomogeneous dispersion. No significant change in the values of Zeta potential at various solid concentrations. By decreasing the solid concentration to be 0.5 mg/ml, the particle interaction can be weakened to produce precise particle size. Based on these, all particle concentration was diluted with water to approximately 0.5 mg/ml. Each sample was measured at 25 °C in triplicate. PCS yields the volume weighted mean particle size and the polydispersity index (PI) of the liquid nanocrystals.

### 2.4. In vitro dissolution studies

Dissolution tests (six replicates) of the baicalein nanocrystal (equivalent to 10 mg baicalein) were performed in 0.1 mol/l hydrochloric acid, pH 4.5 phosphate buffer and pH 6.8 phosphate buffer (37 °C, $V$ = 900 ml) using the USP 2 dissolution apparatus (Sotax A7 Dissolution Apparatus: Sotax Ltd, London, UK) with the paddle rotating at 100 rpm. The baicalein crystal and the physical mixture (PM) containing the same ingredients with the similar ratio in the baicalein nanocrystal were also tested for comparison. Samples (2 ml) were withdrawn and filtered for analysis at specified time points, and assessed for baicalein content by HPLC (Shimadzu Corporation, Japan). For analysis, a reversed phase Shimadzu-pack VP-ODS C18 (4.6 × 150 mm, 5 μm particles) column in conjunction with a precolumn C18 insert was used and the peaks of interest eluted with mixtures of methanol and 0.05% (v/v) phosphoric acid solution (70:30, v:v). The flow rate of 1.0 ml/min was maintained. The column effluent was monitored at 276 nm. Quantification of baicalein was carried out by measuring the peak areas in relation to those of standards chromatographed under the same conditions.

### 2.5. Scanning electron microscopy

Morphological evaluation of the baicalein crystal and the baicalein nanocrystal was performed by scanning electron microscope (SEM) (Hitachi X650, Tokyo, Japan). All samples were examined on a brass stub using carbon double-sided tape. Powder samples were glued and mounted on metal sample plates. The samples were gold coated (thickness ≈15–20 nm) with a sputter coater (Fison Instruments, UK) using an electrical potential of 2.0 kV at 25 mA for 10 min. An excitation voltage of 20 kV was used in the experiments.

### 2.6. Differential scanning calorimetry (DSC)

The status of crystallinity of the baicalein crystal and the baicalein nanocrystal was characterized with DSC on a Netzsch DSC 204 F1 Phoenix Differential Scanning Calorimeter (Germany) which was calibrated for temperature and cell constants using indium. Samples were placed on non-hermetic aluminium pans. The sample cell was equilibrated at 25 °C and then heated at a rate of 10 °C/min in a range of 30–320 °C. Data analysis was performed using NETZSCH-Proteus software (version 4.2).

### 2.7. X-ray powder diffractometry (XRPD)

X-ray powder diffraction patterns of the baicalein crystal and the baicalein nanocrystal were investigated using a Bruker D8 Advance X-ray powder diffractometer (Karlsruhe, Germany) with Cu-Kα radiation (1.5406 Å). The samples were gently consolidated in an aluminium holder and scanned at 40 kV and 40 mA from 5 to 45° $2\theta$ using a scanning speed of 2°/min and a step size of 0.04°. The diffraction patterns were analyzed using Materials Studio (version 4.0) and OriginPro 7.0 (OriginLab Corporation, USA).

### 2.8. In vivo bioavailability study

#### 2.8.1. Animals

The study was approved by the Ethical Committee of China Pharmaceutical University. Male Sprague-Dawley rats (220 ± 10 g) were purchased from Qinglongshan Animal Center (Nanjing, China). All animals were fasted for 12 h prior to drug administration and water was freely available. All animals were housed individually in standard cages on a 12 h light–dark cycles, were fed with standard animal chow daily, and had free access to drinking water. All animals used in this study were handled in accordance with the guidelines of the Principles of Laboratory Animal Care (State Council, revised 1988).

#### 2.8.2. Experimental protocol

The body weight of each rat was measured before drug administration. Before oral administration to the rats, the baicalein crystal or the baicalein nanocrystal was dispersed homogeneously in 0.5% CMC-Na aqueous solution to get the suspension of 10.65 mg/ml. For intravenous injection of baicalein, baicalein was dissolved in PEG400 aqueous solution (50%) to get a solution of 2.2 mg/ml. For pulmonary administration of the baicalein crystal, baicalein crystal was sieved through 100 mesh sieve and was dispersed in water to get the homogeneous dispersion of 4.4 mg/ml. For pulmonary administration of the baicalein nanocrystal, solid nanocrystal was dispersed in water to get the homogeneous dispersion of 4.4 mg/ml.

Male Sprague-Dawley rats (body weight: 250–280 g) were anesthetized with an intramuscular injection of a mixture containing ketamine (80 mg/kg) and xylazine (8 mg/kg). Right jugular vein for blood sampling was cannulated with a polyethylene tubing (0.5 mm ID, 1 mm OD, Portex Ltd., Hythe, Kent, England), filled with a heparin saline solution (50 U/ml). The rats were fasted for at least 12 h prior to the administration and they were not in anesthetized state so 12 h was necessary for them to recover (Aghazadeh-Habashi and Jamali, 2008; Lin and Ho, 2009).

Rats were allocated at random to four groups (6 rats in each group). For oral administration, two groups received gavage administration of the baicalein crystal suspension and the baicalein nanocrystal at a dose of baicalein (121 mg/kg b.w. expressed as baicalein equivalents). For intravenous injection of baicalein, the intravenous bolus was given to rats via the tail vein at a dose of 10 mg/kg. For pulmonary administration of the baicalein nanocrystal (10 mg/kg), the rats were anesthetized by pentobarbital (45 mg/kg, i.p.), rested on its back on an animal board and its limbs were secured, lighted by a red electric light bulb (100 W) hanging over the animals at a distance of about 25 cm to keep its body temperature constant during the experiment. After the trachea was exposed through a longitudinal incision along the ventral aspect of the neck, an incision was made between the fifth and sixth tracheal rings caudal to the thyroid cartilage. Then a microsyringe with metal tubing (0.9 mm in diameter) was inserted through the incision. The aqueous dispersion of the baicalein nanocrystal (~100 μl) at 37 °C was instilled into rat's lung through the blunt needle of a calibrated 250 μl syringe (Microliterÿno. 725, Hamilton Co., Reno, USA). The needle was inserted through the tracheal cannula to a depth of 2.5 cm below the tracheal incision for the injection. At this distance of insertion, the tip of the syringe needle was located 1–2 mm above the bifurcation of the trachea. The rat was adjusted to an angle of 80° before completing the administration of the nanocrystal dispersion over a period of 1–2 s. Immediately thereafter, the microsyringe was withdrawn completely while keeping the angle for 1 min. Then the animal was returned to an angle of 10° (Chen et al., 2002; Katsumi et al., 2010).

After gavage administration of the baicalein suspension and the baicalein nanocrystal, about 200 μl of blood sample was collected from the jugular vein into heparinized tubes at 0, 0.167, 0.5, 1, 1.5, 2, 4, 6, 8, 10, 12, 16 and 24 h. For pulmonary administration of the baicalein crystal, baicalein nanocrystal and intravenous baicalein injection, about 200 μl of blood sample was collected from the jugular vein into heparinized tubes at 0.083, 0.167, 0.333, 0.5, 1, 1.5, 2, 4, 6, 8 and 10 h. Plasma was immediately separated by centrifugation (10 °C, 10 000 × *g*, 5 min) using a refrigerated table top centrifuge (Sigma 1-15K, Sigma, Germany) and kept frozen at −20 °C until analysis.

#### 2.8.3. Determination of baicalin and baicalein

The bioavailability study is based on the determination of baicalin and baicalein in plasma. In this study, a HPLC/UV method was employed to simultaneously determine the concentration of baicalin and baicalein in rat plasma using a reversed phase HPLC (Shimadzu LC 10AD, Shimadzu Corporation, Kyoto, Japan). Baicalin and baicalein were separated by a C18 column (Shimadzu VP-ODS column, 150 mm × 4.6 mm) guarded with a precolumn (Shimadzu) and detected at 276 nm. The mobile phase consisted of methanol and 0.2% phosphoric acid aqueous solution in a volume ratio of 57/43. The mobile phase was pumped at a flow rate of 1.0 ml/min.

The extraction procedure was as follows: 100 μl of rat plasma was mixed with 50 μl of potassium dihydrogen phosphate buffer (0.5 mol/l, containing 1% sodium ascorbate) and mixed for 2 min (Gong et al., 2008). Then, the plasma samples were extracted with 150 μl acetonitrile by vortex-mixing for 10 min and centrifuged for 10 min (10 °C, 10 000 × *g*). The obtained supernatant was centrifuged for another 5 min (10 °C, 10 000 × *g*). 20 μl supernatant was injected into the HPLC system for analysis as described.

### 2.9. Data analysis

Pharmacokinetic analysis was performed by means of a model independent method using the DAS2.0 computer program (issued by the State Food and Drug Administration of China for pharmacokinetic study). The maximum plasma concentration ($C_{max}$) and the time to reach maximum plasma concentration ($T_{max}$) were directly obtained from plasma data. The area under the plasma concentration–time curves ($AUC_{0-10h}$ or $AUC_{0-24h}$) was calculated using the trapezoidal method.

The bioavailability was calculated according to the following Eq. (1):

$$F_{rel} \text{ or } F_{abs} = \frac{AUC_a/Dose_a}{(AUC_b/Dose_b) \times 100\%} \quad (1)$$

where a or b means the different administration route, $F_{rel}$ is the relative bioavailability, $F_{abs}$ is the absolute bioavailability.

All results were expressed as mean ± S.D. Statistical data analyses were performed using one-way analysis of variance (ANOVA) with $P < 0.05$ as the minimal level of significance.

## 3. Results and discussion

### 3.1. Effects of stabilizer in anti-solvent on particle size

In order to prevent the particles from blocking the gap of the homogenizer, baicalein powder should be micronized before homogenization. Jet mill can also be used to achieve size reduction. However, it was found that jet mill had obvious disadvantages, including the waste of expensive drug material, low processing efficiency and especially producing the powder with strong electrostatic force. After comparison, anti-solvent recrystallization was used as the pre-treatment step before the high energy process. The treatment method can get repeatable micron size (0.5–2 μm) and all baicalein crystal can be used for the next processing.

In order to reduce the free energy of the solvent and anti-solvent system, the appropriate type and concentration of the surfactant in the aqueous phase were usually requisite to achieve smaller particle size and the stable dispersion system. In this study, the concentration of polysorbate, SLS and poloxamer 188 was compared at a level of 0.1–0.5%. As listed in Table 1, the surfactant type and concentration in anti-solvent and homogenization are important parameters influencing the nanocrystal size and polydispersity index. It was found that polysorbate 80 at 0.1%, SLS and poloxamer188 at 0.1% and 0.3% in anti-solvent resulted in a rapid agglomeration, while higher concentration of stabilizer (0.3–0.5% polysorbate 80, 0.5% SLS and 0.5% poloxamer188) could hinder the diffusion between the solvent and anti-solvent during precipitation (Kocbek et al., 2006). Polysorbate 80 had better ability to stabilize the dispersion system at relatively low concentration (0.3%). In the range of 0.1–0.5% (w/v), polysorbate 80 did not affect significantly the values of zeta potential, similar to the nonionic surfactants studied (Petryshyn et al., 2010). Considering the relatively low amount and the enough efficiency, 0.3% polysorbate 80 was chosen as the stabilizer for the preparation of baicalein nanocrystals.

### 3.2. Effects of homogenization parameters on particle size

The mean size of the bulk population obtained during the high pressure homogenization process depends mainly on the power density of the homogenizer and the number of homogenization cycles. Providing the enough given power density by running certain cycles, the mean particle size will became constant (Gao et al., 2010). After several cycles with low pressure homogenization, a subsequent processing at 1000 bar was run. As seen from Table 1, particle size decreased rapidly with the increase in the number of homogenization cycles. After 10 cycles, the particle size decreased to 335 nm (±18 nm) determined by PCS. The optimal number of cycles was found to be 10 cycles with a polydispersity index (PI) of 0.12.

### 3.3. Redispersibility of the nanocrystal

The liquid nanocrystal was transformed into the solid by vacuum desiccator to provide the stable solid form. To investigate the effect of drying process on the redispersibility of the nanocrystal, the particle size analysis of the liquid nanocrystal dispersion before drying and the resulted reconstituted liquid dispersion was performed. It was visually observed that once contacting with the surface of distilled water in a glass bottle, a fast and spontaneous diffusion was observed immediately, even without the vigorous hand-shaking. No sign of accumulation in aqueous environments was observed under microscope even after 5 h. The particle size was determined to be 351 ± 24 nm when the bottle containing the reconstituted mixture was just reversed gently for ten times. It can be found from Table 2 that no significant change was observed in the particle size, polydispersity

**Table 1**
The mean particle size (nm) and the width of the particle size distribution (polydispersity index, PI) of the liquid baicalein nanocrystal prepared using different surfactants and homogenization conditions.

| | 5 × 1000 bar (PI) | 10 × 1000 bar (PI) | 15 × 1000 bar (PI) | 20 × 1000 bar (PI) | 25 × 1000 bar (PI) | 30 × 1000 bar (PI) | 35 × 1000 bar (PI) |
|---|---|---|---|---|---|---|---|
| Polysorbate 80 (0.1%) | – | – | – | – | – | – | – |
| Polysorbate 80 (0.3%) | 392 ± 26 (0.22 ± 0.03) | 335 ± 18 (0.12 ± 0.01) | 327 ± 14 (0.11 ± 0.01) | 320 ± 12 (0.16 ± 0.02) | 322 ± 11 (0.21 ± 0.02) | 319 ± 12 (0.19 ± 0.01) | 324 ± 10 (0.11 ± 0.00) |
| Polysorbate 80 (0.5%) | 378 ± 28 (0.25 ± 0.03) | 328 ± 14 (0.13 ± 0.01) | 322 ± 16 (0.22 ± 0.02) | 306 ± 12 (0.21 ± 0.03) | 292 ± 8 (0.11 ± 0.00) | 287 ± 5 (0.09 ± 0.00) | 293 ± 4 (0.19 ± 0.01) |
| SLS (0.1%) | – | – | – | – | – | – | – |
| SLS (0.3%) | – | – | – | – | – | – | – |
| SLS (0.5%) | 367 ± 31 (0.27 ± 0.02) | 343 ± 18 (0.26 ± 0.02) | 332 ± 13 (0.14 ± 0.01) | 313 ± 8 (0.22 ± 0.01) | 304 ± 6 (0.32 ± 0.01) | 297 ± 4 (0.19 ± 0.01) | 301 ± 4 (0.18 ± 0.00) |
| Poloxamer 188 (0.1%) | – | – | – | – | – | – | – |
| Poloxamer 188 (0.3%) | – | – | – | – | – | – | – |
| Poloxamer 188 (0.5%) | 353 ± 27 (0.24 ± 0.03) | 342 ± 15 (0.19 ± 0.02) | 335 ± 14 (0.17 ± 0.01) | 324 ± 11 (0.14 ± 0.01) | 319 ± 8 (0.13 ± 0.01) | 309 ± 7 (0.18 ± 0.02) | 313 ± 5 (0.19 ± 0.02) |

–, agglomerated.

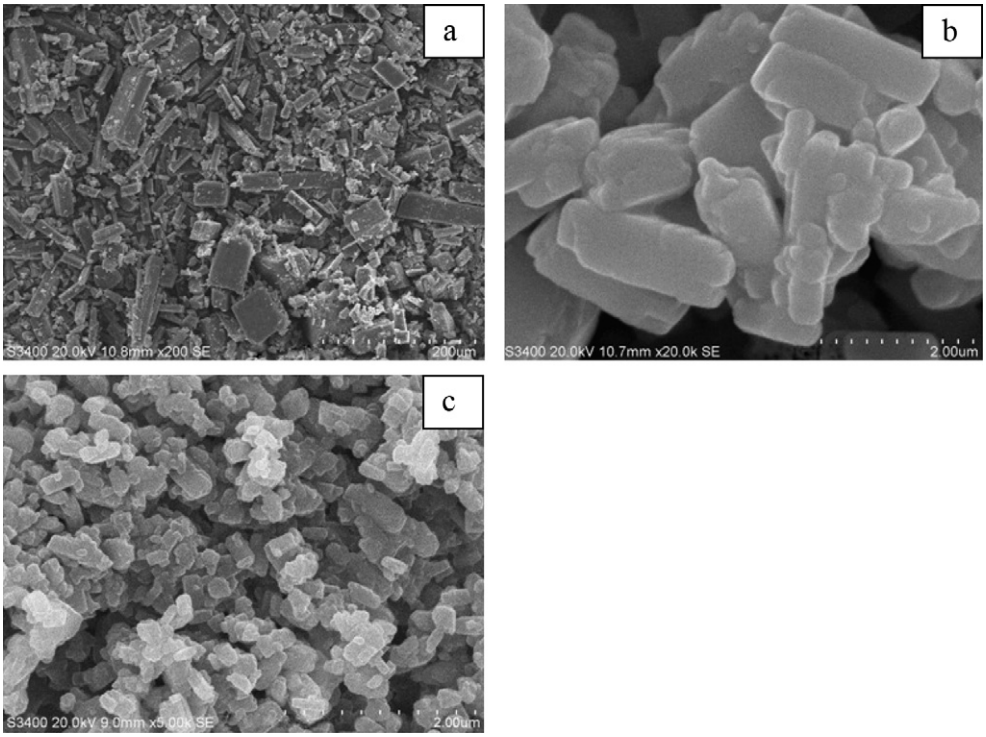


**Fig. 2.** SEM images of the baicalein crystals (a), baicalein microcrystals gained after anti-solvent recrystallization process (b) and baicalein nanocrystals produced by the subsequent high pressure homogenization (c).

index and Zeta potential. The diameter of resulted dispersion was determined by PCS to be 346 ± 22 nm, a similar particle size to the mean of the fresh liquid nanocrystal (335 ± 18 nm), which indicated that the surfactant is sufficient to stabilize the nanocrystal during the preparation and reconstitution process. At the optimized concentration, polysorbate 80 would keep surrounding the nanocrystal surface during anti-solvent recrystallization and homogenization. The vast majority of polysorbate 80 was removed by centrifugation. However, a certain amount of polysorbate 80 adhered to the surface of solid nanocrystals will precipitate together with the nanocrystals during centrifugation and form a solid coverage layer outside the nanocrystalline particles after drying, which could make the nanocrystal finely redispersed in the water. Compared to the Zeta potential of baicalein aqueous dispersion without any additive (+5.12 ± 1.02 mV), the negative Zeta potential of baicalein nanocrystal (−32.55 ± 2.15 mV) resulted from re-dissolved polysorbate 80 in deionized water can be beneficial to the good redispersibility of solid nanocrystals.

### 3.4. Scanning electron microscopy

Morphology assessment of particles using SEM helped to exhibit the morphological changes of baicalein after the size reduction process. As seen from Fig. 2, anti-solvent recrystallization and high pressure homogenization process obviously modified the shape and size of baicalein.

**Table 2**
The characteristics of the baicalein nanocrystals before drying and after reconstitution (means ± S.D., $n = 3$).

| | Before drying | After reconstitution |
|---|---|---|
| Particle size (nm) | 335 ± 18 | 346 ± 22 |
| Polydispersity index (PI) | 0.12 ± 0.02 | 0.15 ± 0.03 |
| Zeta potential (mv) | −34.76 ± 2.63 | −32.55 ± 2.15 |

The baicalein crystals showed irregular long-strip shape with particle size ranging from 20 to 160 μm (Fig. 2a). After the anti-solvent recrystallization process, the baicalein microcrystal presented the cylindrical shape, with smooth surfaces and particle size about 0.5–2 μm (Fig. 2b). Through the anti-solvent recrystallization process, the particle size decreased significantly without the use of jet mill or other intense mechanical force, demonstrating the good performance of anti-solvent recrystallization as the pre-treatment process. The micrograph of the baicalein nanocrystal produced by the subsequent high pressure homogenization indicated homogenous particle distribution with the particle size of 200–400 nm (Fig. 2c). The ratio of length and width of the cylindrical particles was significantly decreased compared to those microcrystals.

It was found previously that the spray dried nanosuspension containing large amount of carrier presented more spherical particles with a "hairy" surface which was the solidified soluble excipients in the formulation (Gao et al., 2010; Mauludin et al., 2009b). As a comparison, almost no solidified excipients (polysorbate 80) could be found at the surface of the nanocrystals, indicating that the processing did not alter the surface morphology of the nanocrystal particles while changing microcrystals into nanocrystals.

### 3.5. In vitro dissolution studies

Standard in vitro nanocrystal powder dissolution testing was used to provide a comparison with the dissolution profiles of baicalein crystal and the PM powder. By HPLC, baicalein was separated well from dissolution media, with retention time of 5.42 min. In the concentration range of 0.5–50 μg/ml, peak area of baicalein correlated well to its concentration ($X$): $Y = 5296.049X - 1252.759$ ($r = 0.9998$, $n = 6$). The limit of quantification and limit of detection for baicalein were 15.2 and 4.8 ng/ml. At concentrations of 2.5, 12.5 and 50 μg/ml, the recoveries of baicalein were 101.2%, 99.93% and

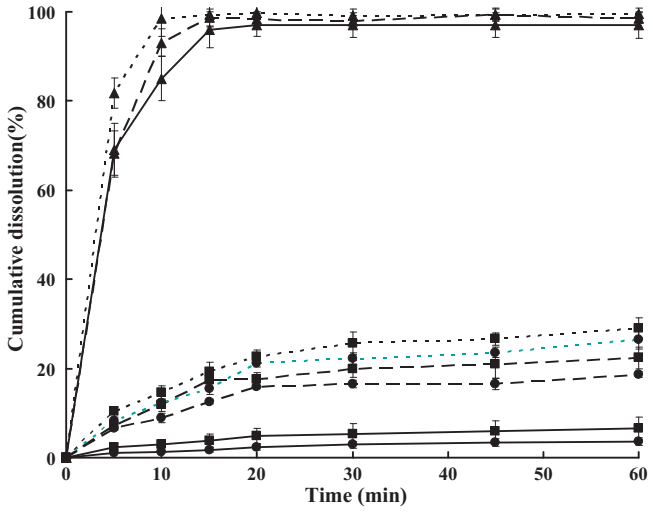


**Fig. 3.** Dissolution profiles for baicalein crystal (●), physical mixture (■) and baicalein nanocrystal (▲) in 0.1 M HCl (solid line), pH 4.5 phosphate buffer (dash line) and pH 6.8 phosphate buffer (dot line). Each value represents mean from six experiments.

99.46%; intra-day precision was 5.20%, 1.43%, and 1.95%; inter-day precision was 5.06%, 1.96%, and 1.15%. The limit of quantification and limit of detection for baicalein were 15.2 and 4.8 ng/ml, respectively.

The nanocrystal powder achieved a very rapid and pH-independent dissolution in three media, with more than 70% baicalein released after approximately 5 min and almost 100% baicalein released after 15 min (Fig. 3). As a comparison, the baicalein crystal and the PM exhibited the much slower and an incomplete dissolution profile, although their dissolution was enhanced in pH 4.5 and 6.8. The maximum dissolution amount of the PM in pH 6.8 buffer was only 29.1% in 60 min. A slight higher dissolution can be observed from the dissolution profiles of the PM, which may be attributed to the wetting action of polysorbate in PM. However, no significant difference was found between the baicalein crystal and the PM ($P > 0.05$). They achieved the similar incomplete dissolution amount ($P > 0.05$). The additives contained in PM had no significant effect on the dissolution of baicalein.

Without the help of large amounts of soluble excipients wrapped around the spherical particle, which may dissolve rapidly to form a hydrophilic wetting environment and to cause the rapid dispersion of nanosuspension in media (Gao et al., 2010), nanocrystal containing very small amount of additives demonstrated the good performance in dissolution as well. The mechanism for enhancing the dissolution may be discussed according to Noyes–Whitney principle (Tong, 2000). The drug dissolution rate is linearly proportional to the surface area exposed to the dissolution medium. The enhancement of dissolution rate can be attributed to the higher surface area of nanocrystals available for dissolution and the decreased diffusion layer thickness (Kesisoglou et al., 2007). These promising results in drug release studies promoted us to perform in vivo studies in rats.

### 3.6. Differential scanning calorimetry (DSC)

DSC thermograms of the baicalein crystal and the baicalein nanocrystal were studied to determine the potential change in the crystalline state of baicalein after the formulation process. As shown in Fig. 4, DSC thermograms for the baicalein crystal and the solid baicalein nanocrystal were identical, with a single sharp endothermic peak, attributing to the melting point of baicalein at 271 °C.

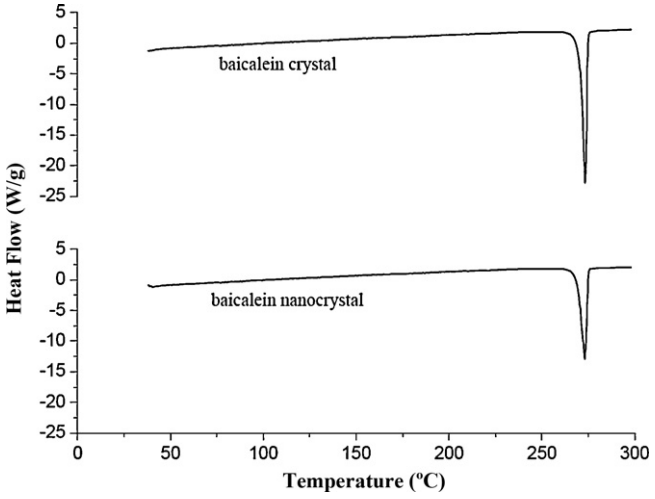


**Fig. 4.** DSC thermograms of baicalein crystal and the baicalein nanocrystal.

### 3.7. X-ray powder diffractometry (XRPD)

XRPD analysis was performed to analyze potential changes in the inner structure of baicalein crystals. The XRPD patterns for baicalein crystal and baicalein nanocrystal are presented in Fig. 5. It can be observed that the characteristic peaks in X-ray diffraction pattern of the baicalein nanocrystal are the same as that of baicalein crystal, indicating the same crystalline form. The identical $2\theta$ peaks at 10.07°, 11.30°, 13.22°, 15.36°, 16.33°, 24.16° and 26.80° appeared at both XRPD. Considering the DSC and XRPD patterns, it can be demonstrated that the crystalline state was apparently unaltered by the use of polysorbate 80 and the anti-solvent recrystallization-high pressure homogenization process, which could ensure the better physicochemical stability.

### 3.8. Bioavailability enhancement

To confirm the usefulness of nanocrystal in improving the oral bioavailability of baicalein, an in vivo test was carried out in rats and pharmacokinetic parameters of the baicalein crystal and the baicalein nanocrystal after gavage administration were compared.

A modified HPLC was established for the simultaneous determination of baicalin and baicalein. Baicalin and baicalein were separated well from impurities in plasma extracts, with retention times of 4.6 min and 11.2 min, respectively. In the concentration

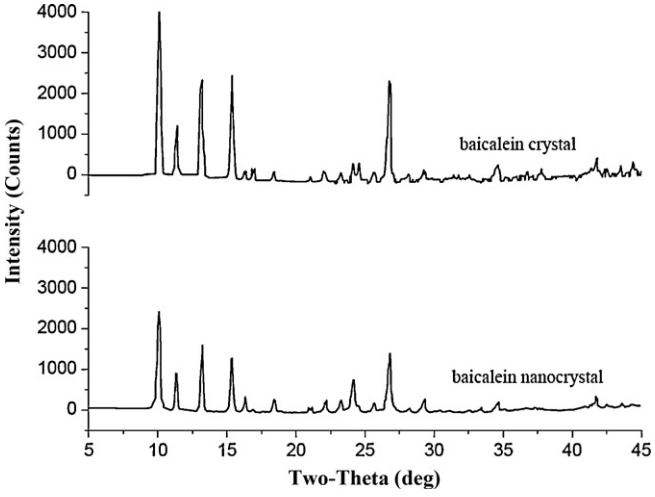


**Fig. 5.** XRPD patterns of baicalein crystal and the baicalein nanocrystal.

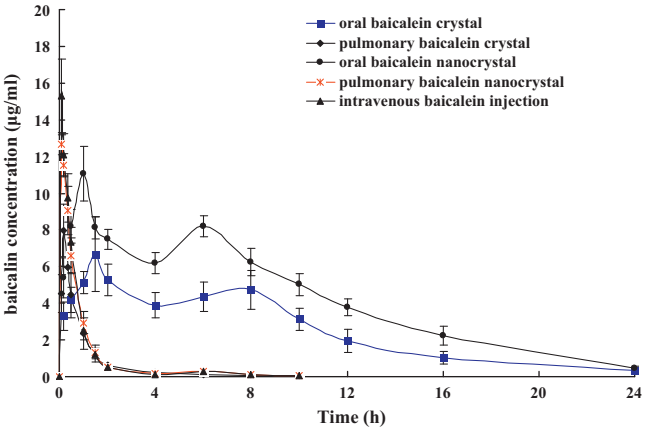


**Fig. 6.** Plasma baicalin concentration–time curves of the baicalein crystal and the baicalein nanocrystal after oral administration to the rats (121 mg/kg), intravenous baicalein injection (10 mg/kg), pulmonary baicalein crystal (10 mg/kg) and pulmonary baicalein nanocrystal (10 mg/kg). Data are expressed as means ± S.D ($n$ = 6).

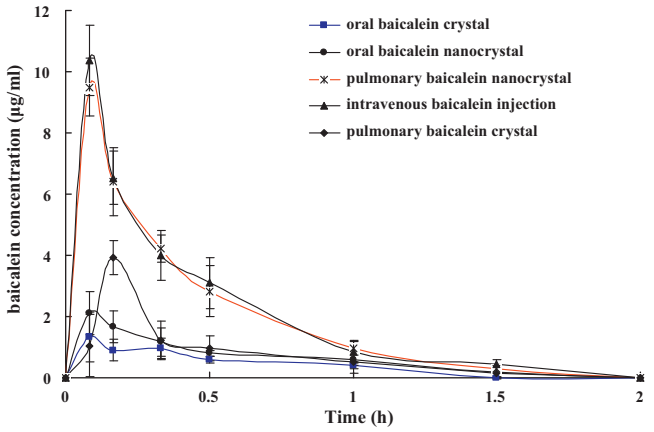


**Fig. 7.** Plasma baicalein concentration–time curves of the baicalein crystal and the baicalein nanocrystal after oral administration to the rats (121 mg/kg), intravenous baicalein injection (10 mg/kg), pulmonary baicalein crystal (10 mg/kg) and pulmonary baicalein nanocrystal (10 mg/kg). Data are expressed as means ± S.D ($n$ = 6).

range of 0.04948–24.74 μg/ml, peak area of baicalin correlated well to spiked plasma concentration ($X$): $Y = 4107.248X - 50.417$ ($r = 0.9986$, $n = 6$). After storage for 15 days at −20 °C and freeze-thawing for three times, baicalin was stable in plasma. The limit of quantification and limit of detection were 40.23 and 13.12 ng/ml, respectively; At concentrations of 0.4948, 4.948 and 14.844 μg/ml, spiked recoveries of baicalin from rat plasma were 104.3%, 97.22%, 98.55%; intra-day precision was 1.23%, 1.06%, 1.46%; inter-day precision was 1.52%, 2.37%, 2.59%.

The preliminary test showed that the maximum plasma baicalin concentration in pulmonary group and intravenous group at the dose of 121 mg/kg was about 230-310 μg/ml. However, the mean spiked recovery of baicalin from rat plasma at 309.25 μg/ml was as low as 66.34%, which may be due to the incomplete extraction of baicalin. So after the conversion based on the maximum blood concentration, the dose in pulmonary group and intravenous group was reduced to 10 mg/kg to ensure the precision and accuracy of the bioavailability studies.

In the concentration range of 0.1425–14.25 μg/ml, peak area of baicalein correlated well to spiked plasma concentration ($X$): $Y = 3799.81X - 235.88$ ($r = 0.9982$, $n = 6$). After storage for 15 days at −20 °C and freeze-thawing for three times, baicalein was stable in plasma. The limit of quantification and limit of detection were 36.12 and 12.45 ng/ml, respectively. At concentrations of 0.7422, 1.425 and 7.125 μg/ml, spiked recoveries of baicalein from rat plasma were 95.70%, 98.02%, 97.43%; intra-day precision was 3.72%, 2.89%, and 2.53%; inter-day precision was 4.72%, 2.81% and 3.22%.

The mean plasma concentrations of baicalin and baicalein *versus* time profiles are shown in Figs. 6 and 7, respectively. From the first sampling time (15 min) after gavage administration to the ending point (24 h), the concentration of baicalin and baicalein in the nanocrystal group was significantly higher than that in the baicalein suspension ($P < 0.05$). It was also found that baicalin was detectable during 24 h and baicalein could not be detected after 2 h. Considering that the absorbed baicalein in the body will restore to baicalin (Akao et al., 2000), all AUC data below were calculated from the plasma concentration of baicalin. Mean pharmacokinetic parameters for the baicalein crystal and the baicalein nanocrystal are listed in Table 3. The baicalein nanocrystal had a significantly lower time to reach the maximum concentration of baicalin than the baicalein crystal. Calculated on $AUC_{0-24h}$, the mean relative bioavailability of baicalein nanocrystal was 1.67-fold that of baicalein crystal.

Several factors could be involved in the improvement of oral baicalein bioavailability. The decreased particle size may increase the dissolution rate by increasing the surface area as elaborated in the Noyes–Whitney equation (Tong, 2000). It was reported that reducing the particle size from 20–30 μm to 270 nm led to faster absorption of naproxen (Liversidge and Conzentino, 1995). In addition, decreased particle size and increased surface area can lead to increased muco-adhesion, which can increase gastrointestinal transit time and lead to increased bioavailability (Rabinow, 2004). After oral dosing of the baicalein crystal and the baicalein nanocrystal, their individual kinetic curve of baicalin both exhibited double peaks, the existence of enterohepatic circulation of baicalin and baicalein might be the reason (Xing et al., 2005).

Compared to the in vitro dissolution difference between baicalein crystal and nanocrystal, the difference between them in in vivo absorption was much less. Several reasons may be involved. After oral administration, the relative fat environment in gastrointestinal tract will enhance the dissolution of lipophilic baicalein. Extensive liver and intestinal first-pass metabolism (Zhang et al., 2005, 2007a,b) and enterohepatic circulation (Xing et al., 2005) may also weaken the effect of dissolution.

The pharmacokinetics of intravenous baicalein injection and pulmonary baicalein nanocrystal at the equivalent dose to rats were also investigated and pulmonary baicalein crystal was studied as a comparison. The mean plasma concentrations of baicalin and baicalein *versus* time profiles are shown in Figs. 6 and 7, respectively. Mean pharmacokinetic parameters for intravenous baicalein injection and pulmonary baicalein nanocrystal are listed in Table 3. Unlike oral administration of baicalein crystal and baicalein nanocrystal, plasma baicalein concentration–time curves of baicalein and baicalin for the intravenous injection and pulmonary baicalein demonstrated to be single peak. Calculated on $AUC_{0-10h}$ of baicalin, the absolute bioavailability of pulmonary baicalein was 49.03% for crystal and 90.81% for nanocrystal. The bioavailability was significantly enhanced by nanocrystallization. There was no significant difference in the pharmacokinetic parameters between the pulmonary baicalein nanocrystal and intravenous baicalein injection ($P > 0.05$). The disappearance of double peaks and the rapid and extensive absorption can be attributed to the absence of first pass effect and enterohepatic circulation.

Compared to the oral baicalein nanocrystal, pulmonary baicalein nanocrystal demonstrated a significantly faster onset time and higher concentration of baicalein and baicalin. Even at a 8.26% administration dose (10 mg/kg), pulmonary baicalein nanocrystal realized the similar baicalin $C_{max}$ to oral baicalein nanocrystal. Larger concentration of drug would occur more rapidly

**Table 3**
Pharmacokinetic parameters from the plasma concentration of baicalin and baicalein in rats after oral administration of baicalein crystal and baicalein nanocrystals (121 mg/kg), intravenous baicalein injection (10 mg/kg), pulmonary baicalein crystal (10 mg/kg) and pulmonary baicalein nanocrystal (10 mg/kg).

| Formulation | Baicalin | | | Baicalein | | |
|---|---|---|---|---|---|---|
| | $T_{max}$ (h) | $C_{max}$ (μg/ml) | $AUC_{0-t}$ (μg h/ml) | $T_{max}$ (h) | $C_{max}$ (μg/ml) | $AUC_{0-t}$ (μg h/ml) |
| Oral baicalein crystal (121 mg/kg) | 1.67 ± 0.29 | 7.18 ± 1.25 | 71.41 ± 4.38 | 0.167 ± 0 | 1.24 ± 0.78 | 0.79 ± 0.08 |
| Oral baicalein nanocrystal (121 mg/kg) | 0.92 ± 0.38[a] | 11.12 ± 1.25[a] | 119.25 ± 20.26[b] | 0.167 ± 0 | 2.10 ± 1.03[a] | 1.25 ± 0.18[a] |
| Intravenous baicalein injection (10 mg/kg) | 0.083 ± 0[b] | 16.66 ± 0.54 | 14.91 ± 0.55 | 0.083 ± 0 | 10.43 ± 1.16 | 4.03 ± 0.85 |
| Pulmonary baicalein crystal (10 mg/kg) | 0.139 ± 0.04[d] | 7.97 ± 1.32[d] | 7.31 ± 0.68[d] | 0.139 ± 0.04[d] | 1.93 ± 0.65[d] | 1.40 ± 0.26[d] |
| Pulmonary baicalein nanocrystal (10 mg/kg) | 0.083 ± 0[b,c] | 15.31 ± 2.01[c] | 13.54 ± 1.03[c] | 0.083 ± 0[c] | 9.52 ± 0.94[c] | 3.88 ± 0.63[c] |

Values are expressed as mean ± S.D. from six experiments. $T_{max}$: time to the maximum concentration; $C_{max}$: the maximum concentration; AUC: area under the curve of plasma concentration *versus* time from $t = 0–24$ h (oral administration) or $t = 0–10$ h (intravenous and pulmonary administration).
[a] $P < 0.05$ *versus* oral baicalein crystal.
[b] $P < 0.01$ *versus* oral baicalein crystal.
[c] $P > 0.05$ *versus* intravenous baicalein injection.
[d] $P < 0.05$ *versus* pulmonary baicalein nanocrystal.

in the lung, leading to higher local drug levels at the absorption site (Jacobs and Müller, 2002). The adhesiveness of nano-sized particles onto surfaces had the tendency to stick to mucosal surfaces at the absorption site over an extended period of time, thus achieving an enhanced absorption rate. The prolonged residence time at the site of absorption would also be beneficial for the increase in the uptake of baicalein, by decreasing the transported amount out of the lungs by cilia movement (Hickey, 1992) and adhering a longer time onto the mucosal surface (Ponchel et al., 1997), thus enhancing the absolute bioavailability from 66.10% of oral nanocrystal to 90.81%, or a relative bioavailability of 137.4% compared to oral nanocrystal. As a water-insoluble bioactive flavonoid, baicalein can be administered intravenously or pulmonarily to gain high bioavailability. From a clinical point of view, pulmonary baicalein nanocrystal can overcome the formulation challenges and has several potential advantages to intravenous baicalein in the prehospital setting, in the clinic, in the emergency department, and even in layperson applications. It may be better the administration of baicalein. Chronic injection is an unpleasant prospect with potential side effects and a host of hygiene issues. Pulmonary delivery may eliminate the barrier to patient compliance caused by injection, while realizing the particular drug regimen required for disease treatment (Michael, 2006).

## 4. Conclusions

Baicalein nanocrystal was prepared by the combination of antisolvent recrystallization and high pressure homogenization. No substantial crystalline change was observed after nanocrystal formation. Compared to the inclusion or solid dispersion method using large amounts of cyclodextrin or polymers to form amorphous baicalein, the baicalein nanocrystal containing only trace of stabilizer also exhibited a markedly enhanced dissolution rate and significantly improved oral bioavailability in rats. By pulmonary delivery, the baicalein nanocrystal can further improve the absolute bioavailability to exhibit identical pharmacokinetic parameters to the intravenous baicalein injection. This study provides the great potential to utilize oral or pulmonary nanocrystals as the effective strategy for other flavonoids that exhibit poor absorption from the gastrointestinal tract.

## Acknowledgments

This work was funded by the Technology Platform for New Formulation and New DDS, Important National Science & Technology Specific Projects (No. 2009ZX09310-004), the Natural Science Projects of Jiangsu Province (No. SBK20080571) and Important National Science & Technology Specific Projects (No. 2011ZX09201-101-02).

## References

Aghazadeh-Habashi, A., Jamali, F., 2008. Pharmacokinetics of meloxicam administered as regular and fast dissolving formulations to the rat: influence of gastrointestinal dysfunction on the relative bioavailability of two formulations. Eur. J. Pharm. Biopharm. 70, 889–894.
Akao, T., Kawabata, K., Yanagisawa, E., Ishihara, K., Mizuhara, Y., Wakui, Y., Sakashita, Y., Kobashi, K., 2000. Baicalin, the predominant flavone glucuronide of *Scutellaria radix*, is absorbed from the rat gastrointestinal tract as the aglycone and restored to its original form. J. Pharm. Pharmacol. 52, 1563–1568.
Amidon, G.L., Lennernas, H., Shah, V.P., Crison, J.R., 1995. A theoretical basis for a biopharmaceutic drug classification: the correlation of in vitro drug product dissolution and in vivo bioavailability. Pharm. Res. 12, 413–420.
Chen, X.J., Zhu, J.B., Wang, G.J., 2002. Hypoglycemic efficacy of pulmonary delivered insulin dry powder aerosol in rats. Acta Pharmacol. Sin. 23, 467–470.
Chou, C.C., Pan, S.L., Teng, C.M., Guh, J.H., 2003. Pharmacological evaluation of several major ingredients of Chinese herbal medicines in human hepatoma Hep3B cells. Eur. J. Pharm. Sci. 19, 403–412.
Collins-Gold, L.C., Lyons, R.T., Bartholow, L.C., 1990. Parenteral emulsions for drug delivery. Adv. Drug Deliv. Rev. 5, 189–208.
Gao, Y., Qian, S., Zhang, J., 2010. Physicochemical and pharmacokinetic characterization of a spray-dried cefpodoxime proxetil nanosuspension. Chem. Pharm. Bull. 58, 912–917.
Gong, M.T., Y, L.F., Chen, Q.H., Xie, B.Y., Lu, W.G., 2008. Study on oral bioavailability of baicalin in rats. Chin. Pharm. J. 43, 1332–1335.
Hickey, A.J., 1992. Methods of aerosol particle size characterization. In: Hickey, A.J. (Ed.), Pharmaceutical Inhalation Aerosol Technology. Marcel Dekker, New York, pp. 219–253.
Hong, T., Jin, G.B., Cho, S., Cyong, J.C., 2002. Evaluation of the anti-inflammatory effect of baicalein on dextran sulfate sodium-induced colitis in mice. Planta Med. 68, 268–271.
Hu, J., Ng, W.K., Dong, Y., Shen, S., Tan, R.B., 2011. Continuous and scalable process for water-redispersible nanoformulation of poorly aqueous soluble APIs by antisolvent precipitation and spray-drying. Int. J. Pharm. 404, 198–204.
Jacobs, C., Müller, R.H., 2002. Production and characterization of a budesonide nanosuspension for pulmonary administration. Pharm. Res. 19, 189–194.
Katsumi, H., Nakatani, M., Sano, J., Abe, M., Kusamori, K., Kurihara, M., Shiota, R., Takashima, M., Fujita, T., Sakane, T., Hibi, T., Yamamoto, A., 2010. Absorption and safety of alendronate, a nitrogen-containing bisphosphonate, after intrapulmonary administration in rats. Int. J. Pharm. 15, 124–130.
Kesisoglou, F., Panmai, S., Wu, Y., 2007. Nanosizing-oral formulation development and biopharmaceutical evaluation. Adv. Drug Deliv. Rev. 59, 631–644.
Kocbek, P., Baumgartner, S., Kristl, J., 2006. Preparation and evaluation of nanosuspensions for enhancing the dissolution of poorly soluble drugs. Int. J. Pharm. 312, 179–186.
Kraft, W.K., Steiger, B., Beussink, D., Quiring, J.N., Fitzgerald, N., Greenberg, H.E., Waldman, S.A., 2004. The pharmacokinetics of nebulized nanocrystal budesonide suspension in healthy volunteers. J. Clin. Pharmacol. 44, 67–72.

Kubo, M., Kimura, Y., Odani, T., Tani, T., Namba, K., 1981. Studies on *Scutellaria radix*. Part 2: the antibacterial substance. Planta Med. 43, 194–201.

Lee, H.Y., Bae, S.M., Kim, K.J., Kim, W., Chung, S.I., Yoon, Y., 2010. β-Catenin mediates the anti-adipogenic effect of baicalin. Biochem. Biophys. Res. Commun. 398, 741–746.

Li-Weber, M., 2009. New therapeutic aspects of flavones: the anticancer properties of *Scutellaria* and its main active constituents Wogonin Baicalein and Baicalin. Cancer Treat. Rev. 35, 57–68.

Lin, H.S., Ho, P.C., 2009. A rapid HPLC method for the quantification of 3,5,4'-trimethoxy-trans-stilbene (TMS) in rat plasma and its application in pharmacokinetic study. J. Pharm. Biomed. Anal. 49, 387–392.

Liu, J., Qiu, L., Gao, J., Jin, Y., 2006. Preparation, characterization and in vivo evaluation of formulation of baicalein with hydroxypropyl-β-cyclodextrin. Int. J. Pharm. 312, 137–143.

Liversidge, G.G., Conzentino, P., 1995. Drug particle size reduction for decreasing gastric irritancy and enhancing absorption of naproxen in rats. Int. J. Pharm. 125, 309–313.

Mauludin, R., Müller, R.H., Keck, C.M., 2009a. Development of an oral rutin nanocrystal formulation. Int. J. Pharm. 370, 202–209.

Mauludin, R., Müller, R.H., Keck, C.M., 2009b. Kinetic solubility and dissolution velocity of rutin nanocrystals. Eur. J. Pharm. Sci. 36, 502–510.

Michael, T.N., 2006. Drug delivery: pulmonary delivery. In: James, S. (Ed.), Encyclopedia of Pharmaceutical Technology. Informa Healthcare, New York, pp. 1279–1286.

Müller, R.H., Gohla, S., Keck, C.M., 2011a. State of the art of nanocrystals – special features, production, nanotoxicology aspects and intracellular delivery. Eur. J. Pharm. Biopharm. 78, 1–9.

Müller, R.H., Shegokar, R., Keck, C.M., 2011b. 20 years of lipid nanoparticles (SLN & NLC): present state of development and industrial applications. Curr. Drug Discov. Technol. 8 (3), 207–227.

Park, S.H., Kwon, J.H., Lim, S.H., Park, H.W., Kim, C.W., 2007. Characterization of human insulin microcrystals and their absorption enhancement by protease inhibitors in rat lungs. Int. J. Pharm. 339, 205–212.

Petryshyn, R.S., Yaremko, Z.M., Soltys, M.N., 2010. Effects of surfactants and pH of medium on zeta potential and aggregation stability of titanium dioxide suspensions. Colloid J. 72, 517–522.

Ponchel, G., Montisci, M.J., Dembri, A., Durrer, C., Duchene, D., 1997. Mucoadhesion of colloidal particulate systems in the gastrointestinal tract. Eur. J. Pharm. Biopharm. 4, 25–31.

Rabinow, B.E., 2004. Nanosuspensions in drug delivery. Nat. Rev. Drug Discov. 3, 785–796.

Shegokar, R., Müller, R.H., 2010. Nanocrystals: industrially feasible multifunctional formulation technology for poorly soluble actives. Int. J. Pharm. 399, 129–139.

Si, D., Wang, Y., Zhou, Y.H., Guo, Y., Wang, J., Zhou, H., Li, Z.S., Fawcett, J.P., 2009. Mechanism of CYP2C9 inhibition by flavones and flavonols. Drug Metab. Dispos. 37, 629–634.

Tong, W.Q., 2000. Preformulation aspects of insoluble compounds. In: Liu, R. (Ed.), Water-insoluble Drug Formulation. Interpharm Press, Denver, Colorado.

Wang, Q., Wang, Y.T., Pu, S.P., 2004. Zinc coupling potentiates anti-HIV-1 activity of baicalin. Biochem. Biophys. Res. Commun. 324, 605–610.

Xing, J., Chen, X., Zhong, D., 2005. Absorption and enterohepatic circulation of baicalin in rats. Life Sci. 78, 140–146.

Yan, F., Ke, X., Ping, Q.N., Wang, J.C., 2008. Preparation of baicalein solid dispersions and oral bioavailability in rats. J. China Pharm. Univ. 39, 406–411.

Yang, D., Hu, H., Huang, S., Chaumont, J.P., Millet, J., 2000. Study on the inhibitory activity, in vitro, of baicalein and baicalin against skin fungi and bacteria. Zhong Yao Cai 23, 272–274.

Zhang, H., Christin, P.H., Zhang, Q., Li, T., 2011. Preparation and antitumor study of camptothecin nanocrystals. Int. J. Pharm. 415, 293–300.

Zhang, H.X., Wang, J.X., Zhang, Z.B., Le, Y., Shen, Z.G., Chen, J.F., 2009. Micronization of atorvastatin calcium by antisolvent precipitation process. Int. J. Pharm. 374, 106–113.

Zhang, L., Lin, G., Chang, Q., Zuo, Z., 2005. Role of intestinal first-pass metabolism of baicalein in its absorption process. Pharm. Res. 22, 1050–1058.

Zhang, L., Lin, G., Kovács, B., Jani, M., Krajcsi, P., Zuo, Z., 2007a. Mechanistic study on the intestinal absorption and disposition of baicalein. Eur. J. Pharm. Sci. 31, 221–231.

Zhang, L., Lin, G., Zuo, Z., 2007b. Involvement of UDP-glucuronosyltransferases in the extensive liver and intestinal first-pass metabolism of flavonoid baicalein. Pharm. Res. 24, 81–89.